IFAI Geosynthetics Conference
Feb. 10-13, 2019 | Houston, TX USA

Factors Affecting Local Stiffness Quantification of Geogrid-Aggregate Interlock Investigated Using Bender Elements

Erol Tutumluer, Ph.D.[1], Joon Han Kim, Ph.D. Candidate[2], Yong-Hoon Byun, Ph.D.[3], Max Orihuela, M.S.[4] and Mark H. Wayne, Ph.D., P.E.[5]

[1]Professor, Paul F. Kent Endowed Faculty Scholar, University of Illinois at Urbana-Champaign, 205 N. Mathews Avenue, Urbana, IL 61801; e-mail: tutumlue@illinois.edu
[2]Graduate Research Assistant, University of Illinois at Urbana-Champaign, 205 N. Mathews Avenue, Urbana, IL 61801; e-mail: kim881@illinois.edu
[3]Assistant Professor, Kyungpook National University, 80 Daehak-ro, Buk-gu, Daegu, 41566, South Korea; e-mail: yhbyun@knu.ac.kr
[4]Graduate Research Assistant, University of Illinois at Urbana-Champaign, 205 N, Mathews Avenue, Urbana, IL 61801; e-mail: morihu4@illlinois.edu
[5]Director of Application Technology, Tensar International Corporation, 2500 Northwinds Parkway No. 500, Alpharetta, GA 30009; e-mail: mwayne@tensarcorp.com

ABSTRACT

This paper focuses on quantifying local stiffness increase near a geogrid when placed and compacted within aggregate specimens. Factors governing the degree of geogrid-aggregate interlocking are investigated through resilient modulus tests, which also incorporate shear wave measurements. Using three pairs of bender elements as shear wave transducers, horizontal shear wave velocities were determined above mid-heights of aggregate specimens where geogrids with two different aperture sizes were installed. The specimens were prepared according to the upper bound and mid-range typical base course gradation band specifications in Illinois at 100%, 95%, and 90% of the maximum dry densities and tested following the standard AASHTO T307 resilient modulus test procedure. The test results show important differences in the stiffness enhancement provided by different geogrid aperture sizes, and influences of gradation and compaction properties on geogrid-aggregate interlocking. Significant densification was observed in loose aggregate specimens of the upper bound gradation when stabilized with geogrids.

INTRODUCTION

Geogrids provide mechanical stiffening in a pavement base course to effectively increase bearing capacity and prevent excessive deformations under vehicular loading. Lateral restraint is the primary stabilization mechanism associated with the interlocking of aggregate particles in the geogrid apertures. Giroud (2009) listed and discussed the governing factors of the interlocking between geogrid and aggregate particles as follows: (i) Aperture size relative to aggregate sizing and grading; (ii) geogrid shape of geogrid aperture; (iii) shape and stiffness of ribs; and (iv) stiffness of ribs and junctions between ribs. Related to the first item above, Jewell et al. (1984) were among the first to highlight the relation between the particle size, geogrid aperture size and the geogrid-aggregate interlocking. Webster (1993) studied further effects of geometry and

physical properties of geogrid on the geogrid-aggregate interlocking. Kwon and Tutumluer (2009) observed a stiffer layer was formed near geogrid due to interlocking between geogrid and aggregate based on the field dynamic cone penetration testing. They used horizontal locked-in residual stresses as an initial condition to assign near geogrid in a sublayer of a granular base for the finite element analyses of their full-scale pavement test sections.

Many researchers have studied the interlocking between geogrid and aggregate using numerical modeling techniques such as the Discrete Element Method (DEM). Konietzky et al. (2004) and McDowell et al. (2006) both indicated that a stiffened, i.e., higher modulus, zone occurred approximately 10 cm above and below the geogrid, expected to vary depending on aggregate size and geogrid type. Zhou et al. (2012) observed the increase in the stiffened zone thickness around geogrid as the applied stress increased. Chen et al. (2014) found that contact forces from aggregate particles increased near geogrid.

Recent research efforts at the at University of Illinois focused on applying shear wave measurement techniques in geogrid stabilized aggregate specimen triaxial tests to quantify stiffness enhancement near geogrid. Byun and Tutumluer (2017) installed two pairs of bender elements at two different heights above a geogrid, which was placed in 1:1 height to diameter ratio specimens, and the results revealed that interlocking of aggregate and geogrid was clearly captured with higher shear wave velocities in the area adjacent to geogrid. Later on, Byun and Tutumluer (2018) installed three pairs of bender elements in 2:1 height to diameter specimens at three different heights above geogrid placed at specimen mid-height, and they quantified stiffness enhancement with measured shear wave velocities to compare the effect of geogrid aperture shape (rectangular and triangular) on geogrid-aggregate interlocking.

Regarding the effect of aggregate grain size distribution on the resilient response and permanent deformation, Mishra and Tutumluer (2012) showed that dense-graded crushed aggregates showed significantly less permanent deformation than gravel specimens, and excessive fines (passing No. 200 sieve size material) caused reduction in shear resistance and resulted in higher permanent deformations for both gravel and the dense-graded crushed aggregate. Similarly, Xiao et al. (2012) represented the particle packing characteristics of aggregate with a new concept of gavel to sand ratio (G/S), and an optimal G/S value was reported for the densest packing. From the aggregate samples of Minnesota Department of Transportation (MnDOT), aggregate materials with G/S of 1.5 gave the highest shear strength.

Kim et al. (2019) recently studied an optimal match between geogrid aperture size and aggregate grain size distribution for geogrid and aggregate interlocking. They installed three sets of bender element pairs on both geogrid stabilized and unstabilized base course aggregate specimens prepared and tested at three different engineered gradations (G/S ratios of 1.0, 1.63, and 2.69) using two different aperture size (33-mm and 40-mm diagonal) triangular geogrids. They found that the mid-range aggregate gradation with a G/S ratio of 1.63 was the closest to the MnDOT optimal aggregate (G/S=1.5) and gave the highest shear wave velocities in the vicinity of geogrid when the aggregate specimen was stabilized with the smaller (33-mm diagonal) aperture size.

OBJECTIVE AND SCOPE

The objective of this paper is to present findings from an ongoing laboratory study at the University of Illinois focused on quantifying the local stiffness increase near a geogrid when placed and compacted in a base course aggregate specimen. The research scope covers

investigating factors governing the degree of geogrid-aggregate interlocking through standard resilient modulus tests, which now also incorporate shear wave measurements using three pairs of bender elements as shear wave transducers. The horizontal shear wave velocities are determined above mid-heights of aggregate specimens where geogrids with two different triangular aperture sizes (GG1 and GG2) are installed and studied for interlocking properties. The aggregate specimens were prepared at upper bound (UB) and mid-range engineered (ENG) gradations of the typical base course gradation band specification of the Illinois Department of Transportation (IDOT). The specimens were prepared at the target 100%, 95%, and 90% of the maximum dry densities (MDD) and tested following the standard AASHTO T307 resilient modulus test procedure.

AGGREGATE MATERIAL STUDIED AND GEOGRID PROPERTIES

Aggregate grain size distributions. A dolomite type aggregate material from a quarry near Fairmont, Illinois was used in this study. The grain size distribution of the aggregate material (source gradation) was determined by dry sieving according to ASTM C136, and it meets IDOT's gradation specifications for CA06 base course materials (see Table 1 and Figure 1). In this study, aggregate samples were prepared to IDOT's CA06 upper bound (UB) and mid-range engineered (ENG) gradations as indicated in Figure 1. To ensure consistent gradations for prepared samples, the aggregate material was size separated into six sizes retained on the sieve sizes shown in Figure 1 (37.5 mm, 25 mm, 12.5 mm, No. 4, No. 16, and No. 200 sieve) by dry sieving. Samples were then prepared to the target gradations (CA06 UB and ENG) by batching materials from the different sizes. Particle size properties such as D_{10}, D_{30}, D_{50}, D_{60}, coefficient of uniformity (Cu), coefficient of curvature (Cc), and gravel to sand (G/S) ratio are summarized in Table 1 for the three gradations (UB, ENG, and LB) and for the original source gradation. The G/S ratio suggested by Xiao et al. (2012) was calculated for each aggregate sample to relate to expected performance, where a G/S ratio closer to 1.5 is the optimum value for highest shear strength. A G/S of 1.63 was calculated for the CA06_ENG gradation, which is slightly greater than the optimum value of 1.5.

Table 1. Grain size properties of Illinois DOT CA06 dense-graded specification.

Illinois DOT CA06 Dense-Graded Specification	D_{10} (mm)	D_{30} (mm)	D_{50} (mm)	D_{60} (mm)	C_u	C_c	Gravel to Sand (G/S) ratio
Upper Bound	0.03	0.46	2.82	5.49	196.6	1.4	1.00
Engineered (mid-range)	0.13	1.73	5.88	8.06	76.5	3.5	1.63
Lower Bound	1.22	4.94	9.27	12.70	10.4	1.6	2.69
Source gradation (as-received from quarry)	0.10	2.08	4.38	6.45	64.5	6.71	1.12

Moisture-density relationships. Compaction tests were conducted for the CA06 aggregate material at the three different gradations (UB, ENG, and LB) to establish the moisture-density relationships. All specimens were compacted at the modified compactive effort as per ASTM

D1557. The optimum moisture content (OMC) and the maximum dry density (MDD) were obtained from the moisture-density curves for each gradation, as follows: (i) UB: OMC=5.9% and MDD=22.84 kN/m^3 (145.6 pcf), (ii) ENG: OMC=5.5% and MDD=22.59 kN/m^3 (143.8 pcf), and (iii) LB, OMC=4.0% and MDD=21.30 kN/m^3 (135.6 pcf).

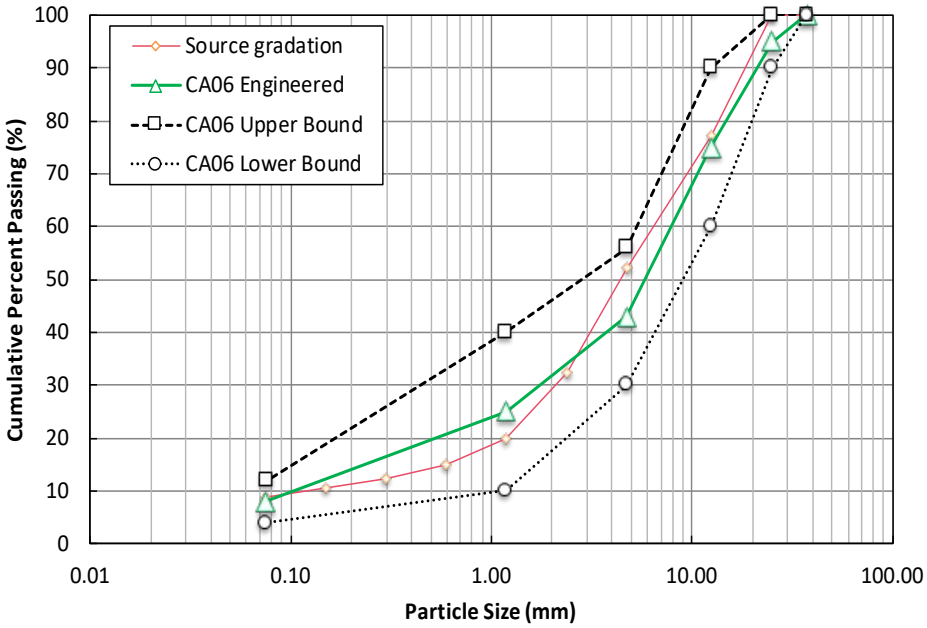

Figure 1. Grain size distribution curves for aggregate materials tested.

Geogrid types and properties. Two punched and drawn geogrids (GG1 and GG2) with triangular apertures were used for stabilizing aggregate specimens, with geogrid placed at the mid-height of the specimen. Detailed information for the dimensions and aperture sizes of these geogrids are given in Table 2. Aperture size can influence the magnitude of the aggregate-geogrid interlocking, depending on the grain size distribution characteristics. Table 2 also lists the sizes of the largest circles that can be inscribed in the triangular aperture, which can be related to the aggregate sizes to provide better geogrid-aggregate interlock for increased mechanical stabilization.

SHEAR WAVE TECHNOLOGY

Shear wave velocity is generally known to be governed by geomaterial's relative density, packing condition, and confining stress thereby representing geomaterial stiffness or shear resistance. In this study shear wave measurement is considered a new approach to quantify geogrid-aggregate interlocking induced mechanical stabilization. To this end, bender element (BE) shear wave technology is applied to resilient modulus testing of unstabilized and geogrid stabilized triaxial specimens.

Bender element shear wave measurement system. Using a pair of BEs, an input signal triggered by a source bender element can travel through a fixed distance (called travel distance) in a dense-graded aggregate material, and the output signal can be then captured by a receiver bender element. Considering the travel distance and time difference between the triggering and

the first arrival of shear wave, the shear wave velocity can be calculated. Each bender element was anchored in a brass mounting base to fix one end of the BE, as shown in Figure 2(a). The BE anchored in the mounting base can trigger the input signal by vibrating like a cantilever beam. To avoid any damage from dynamic impact during the compaction and repeated load triaxial testing, a pair of thick protection bars above and below bender element was extended from the mounting base.

Table 2. Geogrid dimensions and properties.

Index Property	Geogrid #1 (GG1)			Geogrid #2 (GG2)		
	Longitudinal	Diagonal	Transverse	Longitudinal	Diagonal	Transverse
Rib pitch mm (in.)	40 (1.57)	40 (1.57)		33 (1.30)	33 (1.30)	
Mid-rib depth mm (in.)		1.3 (0.051)	1.2 (0.047)		1.6 (0.063)	1.2 (0.047)
Mid-rib width mm (in.)	0.9 (0.035)	1.2 (0.047)	0.4 (0.016)	0.7 (0.028)		
Diameter of largest inscribed circle mm (in.)	23.1 (0.909)			19.1 (0.752)		
Aperture Details (showing largest inscribed circle)	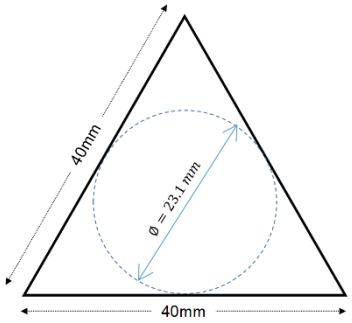			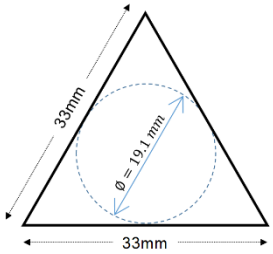		

The shear wave measurement system consisted of a signal generator, pre-amplifier, filter-amplifier, oscilloscope, and computer, as shown in Figure 2(b). A step pulse of 20 Hz and 10V magnitude was generated by the signal generator and transmitted to the pre-amplifier. The input signal was intensified 10 times through the pre-amplifier. After detecting the shear wave at receiver bender element, the output signal was transmitted to the filter-amplifier to remove unintended noise from the signal. The signal to noise ratio of output signal was enhanced by stacking 1,024 recorded signals.

RESILIENT MODULUS TESTS

With two different aperture size geogrids (GG1 and GG2), geogrid stabilized and unstabilized aggregate specimens were prepared for resilient modulus tests. Three pairs of BEs were attached on the surface of membrane at three different positions [top, middle, and bottom; see Figure 2(b)] above the mid-height of specimen. Air leakage was prevented by sealing any gap between the

membrane and mounting base with glue and silicon. Then, the membrane was placed in a split compaction mold. The aggregate specimens were compacted by a rammer with a modified compaction effort of approximately 2,700 kN·m/m^3 (56,391 lb·ft/ft^3). Specimens with 150 mm (6 in.) in diameter and 300 mm (12 in.) height were compacted in six layers with 56 blows per layer. After the compaction of the third layer, a circular geogrid cut (GG1 or GG2) was placed at the mid-height of stabilized specimens.

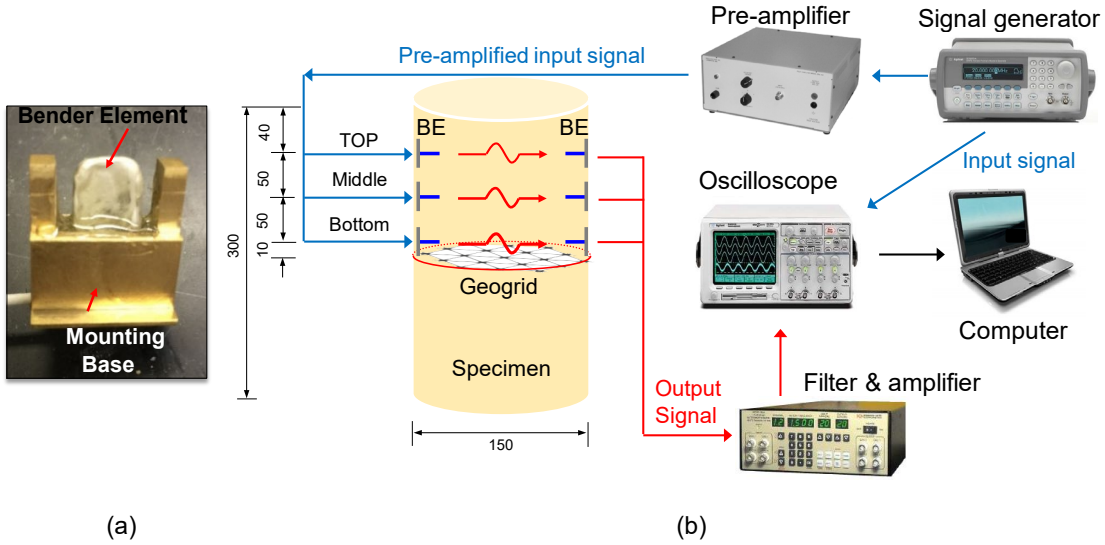

Figure 2. Schematic drawings of test setup: (a) bender element and mounting base; (b) triaxial specimen with shear wave measurement system and bender elements. The unit of the height and diameter of specimen is millimeter.

To study the effect of geogrid type/aperture (GG1 and GG2) and CA06 aggregate gradations on the stiffness enhancement due to interlocking, the target optimum water contents and maximum dry densities were accomplished for the compacted specimens at UB and ENG gradations in the early scope of this study. Further, to study the degree of compaction, CA06 aggregate specimens at the UB gradation were compacted and prepared with GG1 and GG2 geogrids at 100%, 95%, and 90% of MDD values at the same OMC conditions. Totally, eight specimens were prepared and tested using a triaxial testing apparatus, referred to as TX-12, following the AASHTO T307 standard resilient modulus test procedure. First, the specimens were conditioned with 1,000 load repetitions using a deviator stress (σ_d) of 103.4 kPa (15 psi) and a constant confining pressure (σ_3) of 103.4 kPa (15 psi). Next, the fifteen standard AASHTO T307 stress states were applied for conducting the resilient modulus tests. After completing the 100 repetitions for each deviator stress confining pressure combination, the shear waves were measured by using the three BE pairs located above the geogrid at specimen mid-height.

RESULTS AND DISCUSSION

Shear wave velocity is commonly used to estimate the small strain stiffness of granular materials. Figures 3 and 4 show the shear wave velocity measurements obtained as a function of the applied stress states from the UB and ENG gradation aggregate specimens stabilized with GG1 and GG2 geogrids, respectively. Related to the three BE pairs installed on the specimen, “bottom” refers to

within 10 mm (0.4 in.) above the mid-specimen height where geogrid was placed, the "middle" refers to 50 mm (1.96 in.) higher than the "bottom," and the "top" location is also 50 mm (1.96 in.) higher than the "middle" location [see Figure 2(b)]. In general, higher shear wave velocities at almost all bulk stress levels were measured at the bottom level in the vicinity of geogrids than the other two levels due to the geogrid lateral restraint mechanism, and the magnitude of interlocking decreases gradually with distance from geogrid. Such higher shear wave velocities at the bottom level compared to the middle and top is a characteristic trend of much better local stiffening in the vicinity of geogrid and implies improved geogrid-aggregate interlocking. When compared to the finer UB gradation specimens seen in Figures 3(a) and 4(a)], the ENG gradation specimens show much higher shear wave velocities measured at the bottom level [see Figures 3(b) and 4(b)]. Giroud (2009) suggested that the geogrid should fill the void of aggregates, and the geogrid aperture can be regarded as a certain fraction of aggregate size. For the case of ENG gradation, the best interlock was achieved from the smaller aperture GG2 geogrid [see Figure 4(b)]. Accordingly, the ENG gradation with D_{50}=5.88 mm and a G/S ratio of 1.63 (see Table 1) had a much better match with the 33-mm diagonal rib pitch of the GG2 geogrid, which is also supported by the more uniformly distributed contact force network as discussed by Xiao and Tutumluer (2012). Therefore, ENG gradation and GG2 geogrid properly established an improved zone that shows increasing stiffness profiles with bulk stress.

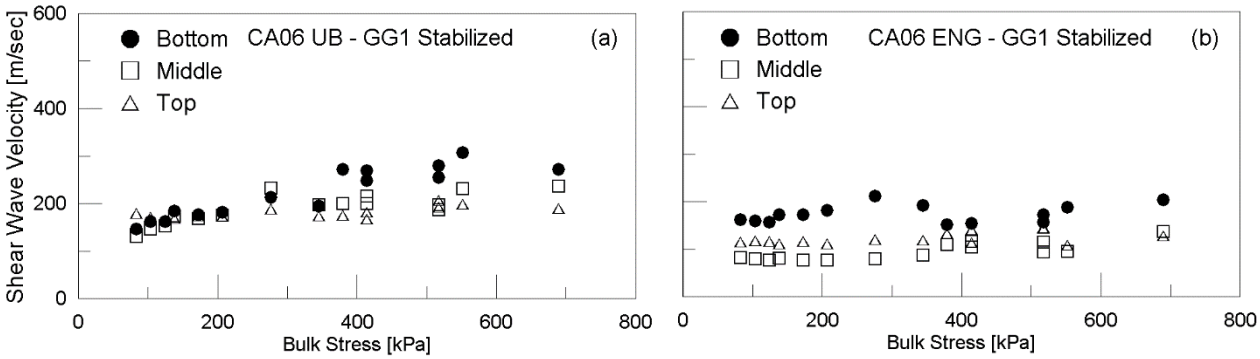

Figure 3. Shear wave velocities graphed with bulk stress for GG1-stabilized aggregate specimens at (a) UB and (b) ENG gradations and achieved 100% MDD conditions.

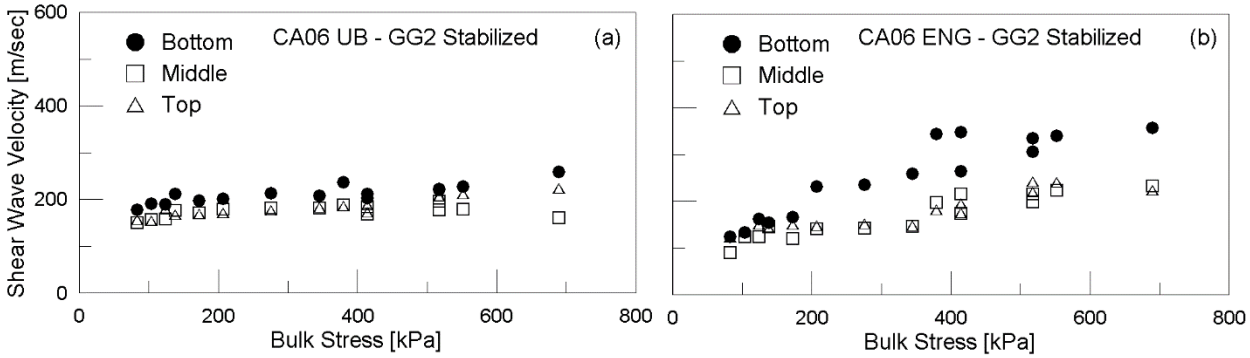

Figure 4. Shear wave velocities graphed with bulk stress for GG2-stabilized aggregate specimens at (a) UB and (b) ENG gradations and achieved 100% MDD conditions.

Note that for unstabilized specimens (no geogrid and no geogrid-aggregate interlock), although not presented in this paper but instead discussed elsewhere (Kim et al., 2019), shear

wave velocities at the top level was generally faster than or similar to those measured at the other levels, likely due to the boundary effect from the load cell on the top of specimens which enhances the resistance to shearing.

Figure 5 shows the effect of achieved specimen density on the shear wave velocities measured in the UB gradation specimens stabilized with GG1 and GG2 geogrids. Three different specimens at 100% of the maximum dry density (MDD), 95% MDD, and 90% MDD were tested in resilient modulus and shear wave testing. Compared to other dry density levels, specimens at 95% MDD showed in general more apparent geogrid-aggregate interlocking and local stiffness enhancement features, especially when stabilized with GG1. The possible explanation is that at 95% MDD, the specimens may be adequately loose and particle mobility is ideal for the geogrid to adequately establish contact force network and better interlock with aggregate particles whereas at 100% MDD, packing condition may be too tight for particles to allow geogrid to establish contact force network. At 90% MDD, specimens may not be uniformly compacted due to the nature of loose condition, hence, interlocking was not established due to lack of the number of contacts between geogrid and aggregate particles. However, one clear trend with geogrid stabilization is that even though geogrid aggregate interlock was missing in some cases, significant overall specimen densification and stiffening took place with much higher shear wave velocities measured in the 95% MDD and 90% MDD specimens when compared to the 100% MDD specimens (see Figure 5).

SUMMARY AND CONCLUSIONS

This paper presented findings from an ongoing research investigation on the use of shear wave technology to determine local stiffness enhancement effects of geogrid stabilized aggregate assemblies. Using bender element (BE) shear wave transducers installed on geogrid stabilized aggregate specimens, factors such as grain size properties, geogrid aperture size, and compaction (achieved dry density) characteristics were investigated on the geogrid-aggregate interlocking induced stiffness enhancement in resilient modulus and shear wave testing. The geogrid stabilized aggregate samples had BE pairs installed at three different levels above mid-height of specimens. Because shear wave velocity is related to geomaterial small strain stiffness through its density and packing condition, and it is a function of applied stress states, shear wave velocity technology can be a reasonable approach for the quantification of geogrid-aggregate interlocking induced stiffness enhancement.

To study grain size distribution effects, samples with two different aggregate gradations, upper bound (UB) and engineered (ENG) mid-range of the Illinois DOT CA06 gradation specification were prepared. Two different triangular aperture size geogrids GG1 (diagonal rib pitch 40 mm) and GG2 (diagonal rib pitch 33 mm) were placed at mid-depth of specimens of the CA06 UB and ENG gradations to investigate the effect of geogrid dimensions. To study compaction properties, UB gradation specimens at 100% of maximum dry density (MDD), 95% MDD, and 90% MDD were prepared with GG1 and GG2 geogrids.

By studying two grain size distributions (CA06 UB and ENG), the ENG gradation specimens showed much higher shear wave velocities measured near the geogrid when compared to the finer UB gradation specimens. An optimal packing condition represented with the ratio of the size fractions of gravel and sand sizes, or gravel to sand (G/S) ratio of 1.63 properly enhanced the geogrid-aggregate interlocking induced local stiffness to indicate a stiffened zone especially in the ENG gradation specimens. This was established based on highest shear velocity

measurements recorded for the smaller aperture GG2 geogrid from the closest BE pair thus indicating an optimal match between geogrid aperture size and grain size distribution.

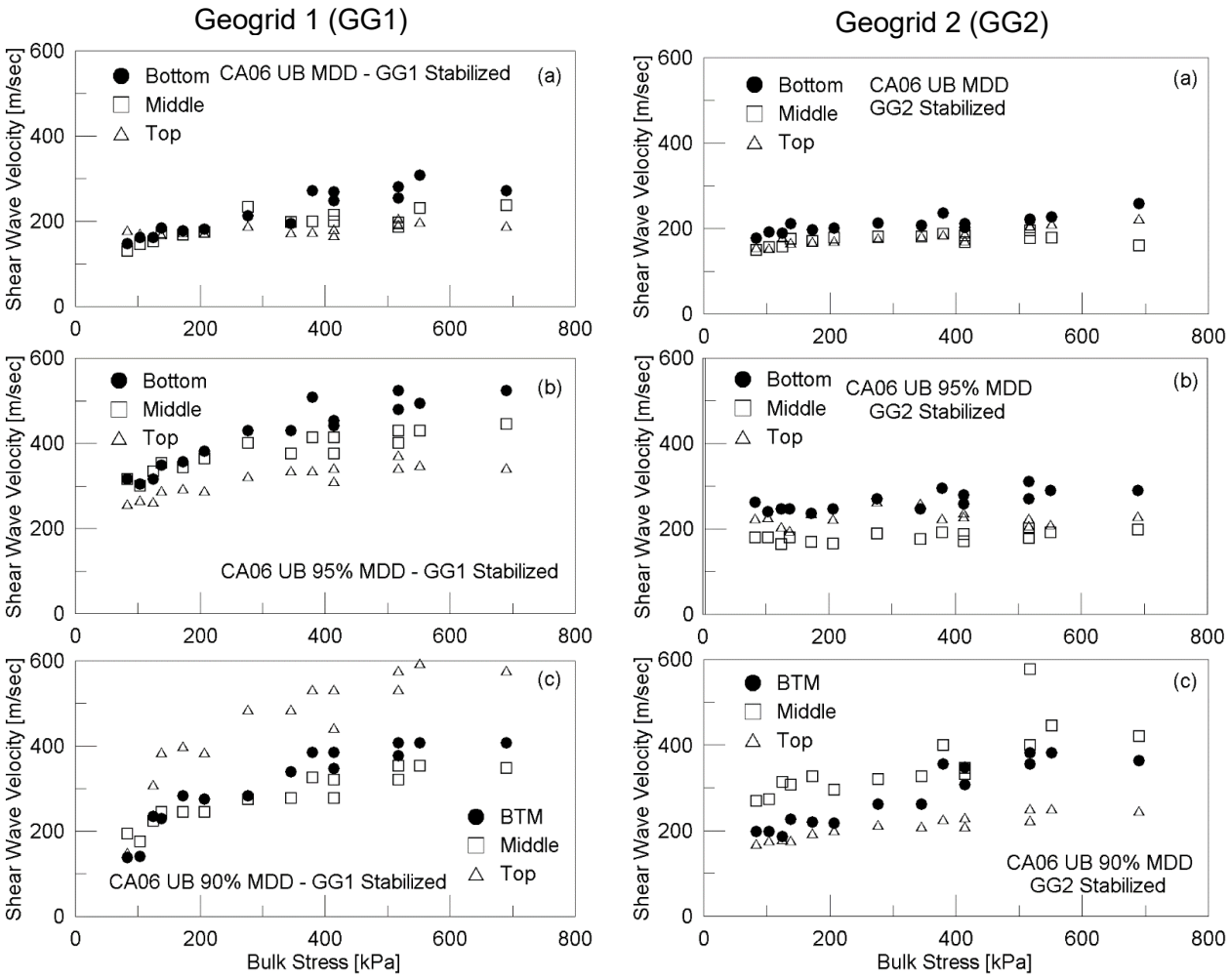

Figure 5. Shear wave velocities graphed with bulk stress for GG1 and GG2 stabilized UB gradation specimens compacted at 100% MDD, 95% MDD, and 90% MDD.

UB gradation specimens stabilized with GG1 and GG2 geogrids were used to study compaction characteristics through three different achieved dry density levels: 100% MDD, 95% MDD, and 90% MDD. Interestingly, only the specimens compacted at 95% MDD indicated an optimal relative density that may provide some mobility of aggregate particles to establish proper interlocking of geogrid and aggregate particles. This was quantified by higher shear wave velocities consistently measured only in the 95% MDD specimens near the installed geogrid. Further, one clear trend with geogrid stabilization was that even though geogrid aggregate interlock was missing in some cases, significant overall specimen densification and stiffening took place with much higher shear wave velocities measured in the 95% MDD and 90% MDD specimens when compared to the 100% MDD specimens.

REFERENCES

Byun, Y. H., and E. Tutumluer. (2017). Bender Elements Successfully Quantified Stiffness Enhancement Provided by Geogrid–Aggregate Interlock. *Transportation Research Record: Journal of the Transportation Research Board*, 2656: 31-39.

Byun, Y. H., E. Tutumluer, B. Feng, J. H. Kim, and M. H. Wayne. (2018). Mechanically Stabilized Layer Characterization due to Geogrid-Aggregate Interlock Using Bender Element Shear Wave Transducers. *Geotextiles and Geomembranes*, (submitted).

Chen, Cheng, G. R. McDowell, and N. H. Thom. (2014). Investigating Geogrid-Reinforced Ballast: Experimental Pull-out Tests and Discrete Element Modelling. *Soils and Foundations,* 54(1): 1–11.

Giroud, J.P. (2009). An assessment of the Use of Geogrids in Unpaved Roads and Unpaved Areas. *Proceedings of the Jubilee Symposium on Polymer Geogrid Reinforcement*, Institution of Civil Engineers, London, UK: 23-36.

Jewell, R. A., G. Milligan, R. W. Sarsby, and D. Dubois. (1984). Interaction between Soil and Geogrids. Polymer Grid Reinforcement. *Proceedings of a Conference sponsored by the Science and Engineering Research Council and Netlon Ltd*, London: 22-23.

Kim J.H., Byun Y.B., Qamhia I.I.A., Orihuela M.F., Tutumluer E., and Wayne M. (2019). Investigation of Aggregate Particle and Geogrid Aperture Sizes for Mechanical Stabilization Using Bender Element Shear Wave Transducers. *Transportation Research Record: Journal of the Transportation Research Board*, Transportation Research Board of the National Academies, Washington, D.C. (submitted).

Konietzky, H., te Kamp, L., Gröger, T. and Jenner, C. (2004). Use of DEM to Model the Interlocking Effect of Geogrids under Static and Cyclic Loading. *Numerical Modeling in Micromechanics via Particle Methods*: Shimizu, Y., Hart, R. and Cundall, P. (Eds.), A.A. Balkema, Rotterdam: 3-12.

Kwon, J., and E. Tutumluer. (2009). Geogrid Base Reinforcement with Aggregate Interlock and Modeling of Associated Stiffness Enhancement in Mechanistic Pavement Analysis. *Transportation Research Record: Journal of the Transportation Research Board*, National Academies, Washington, D.C., No. 2116: 85–95.

McDowell, G.R., Harireche, O., Konietzky, H., Brown, S.F. and Thom, N.H. (2006). Discrete Element Modeling of Geogrid-reinforced Aggregates. Proceedings, Institution of Civil Engineers, Geotechnical Engineering 159: 35-48.

Mishra, D., and E. Tutumluer. (2012). Aggregate Physical Properties Affecting Modulus and Deformation Characteristics of Unsurfaced Pavements. ASCE *Journal of Materials in Civil Engineering*, ASCE, 24(9): 1144-1152.

Webster, S. L. (1993). Geogrid reinforced Base Courses for Flexible Pavements for Light Aircraft: Test Section Construction, Behavior under Traffic, Laboratory Tests, and Design Criteria. *Technical Report. GL-93-6*, U.S. Army Corps of Engineers. Waterways Experiment Station (USAE-WES), Vicksburg, MS.

Xiao, Y., E. Tutumluer, Y. Qian, and J. Siekmeier. (2012). Gradation Effects Influencing Mechanical Properties of Aggregate Base and Granular Subbase Materials in Minnesota. *Transportation Research Record 2267, Journal of the Transportation Research Board*, National Research Council, Washington, D.C.: 14-26.

Zhou, J., J. F. Chen, J. F. Xue, and J. Q. Wang. (2012). Micro-mechanism of the Interaction between Sand and Geogrid Transverse Ribs. *Geosynthetics International*, 19(6): 426–437.